ELSEVIER

Journal of Alloys and Compounds 429 (2007) 198–203

Journal of ALLOYS AND COMPOUNDS

www.elsevier.com/locate/jallcom

Microstructures and mechanical properties of aluminum matrix composites fabricated from Al–x wt.% $Zr(CO_3)_2$ ($x = 5, 10, 15, 20, 25$) systems

Song-Li Zhang, Yu-Tao Zhao*, Gang Chen, Xiao-Nong Cheng, Qi-Xun Dai

School of Materials Science and Engineering, Jiangsu University, Zhenjiang, Jiangsu 212013, PR China

Received 5 April 2006; received in revised form 19 April 2006; accepted 19 April 2006

Abstract

The aluminum matrix composites reinforced by Al_2O_3 and Al_3Zr particulates were fabricated from Al–x wt.% $Zr(CO_3)_2$ ($x = 5$, 10, 15, 20, 25) systems via magneto chemistry in situ reaction at 1173 K. XRD analysis shows that α-Al_2O_3 and Al_3Zr reinforcement phases have been obtained. The microstructure analysis indicates that the reinforcement particulates are distributed uniformly in the aluminum matrix and the size is 0.08–0.12 μm. The mechanical properties test results show that the tensile and yield strengths of the composites are much higher than that of pure aluminium. The values of the tensile, yield strengths and elongations change with x from 5 to 25. Especially when $x = 20$, the composite exhibits the highest tensile and yield strengths with $k_b = 2.151$ and $k_s = 3.298$, reaching 167.8 and 138.5 MPa, respectively.

Keywords: Aluminum matrix composite; Magneto chemistry; Microstructure; Mechanical properties

1. Introduction

In recent years, much work has been done on aluminum metal-matrix composites to meet the increasing demands of advanced structural applications, including aircraft components and key parts in automobiles, such as brake rotors and drums due to their light density, high elastic modulus, specific strength and good thermal stability compared with conventional monolithic alloys [1–5]. Aluminum matrix composites reinforced by particulates can be fabricated by ex situ synthesis, where particles are added to the melt as a powder (e.g. liquid ingot casting and powder metallurgy) [6–9] and in situ synthesis, where particles are synthesized within the melt (e.g. exothermic dispersion, reactive hot pressing, reactive infiltration and direct melt reaction) [10–12]. Especially, direct melt reaction (DMR) process is considered one of the most promising in situ synthesis techniques for commercial applications due to its simplicity, low cost and near net-shape forming capability. However, the DMR process requires long agitating time at high temperature in order to obtain full incorporation and thorough reaction of the added reactants with the molten metal [13]. In order to eliminate the requirement for long mixing time at high temperature, some work has been done [14–18]. Up to the present, the processing technology for the Al–$Zr(CO_3)_2$ composites reinforced by Al_2O_3 and Al_3Zr particles via magnetochemistry in situ melt reaction has not been reported.

In the present work, we focused on a novel and economical technique to fabricate bulk Al–$Zr(CO_3)_2$ composites at 1173 K via magnetochemistry in situ melt reaction. The microstructures and mechanical properties of the composites were investigated.

2. Experimental procedures

The starting materials were commercial aluminum ingots and inorganic salt $Zr(CO_3)_2$ powder (average size 20 μm). Table 1 shows the nominal composition of the experimental $Zr(CO_3)_2$ powder. Firstly, $Zr(CO_3)_2$ powders were dehydrated at 573 K for 3 h in an electric furnace. Then aluminum ingots were heated at 5 °C/min. Fig. 1 shows the schematic diagram of experiment setup. When the temperature of the melt was at 1173 K, the dried $Zr(CO_3)_2$ powders with the weight ratio x ($x = 5$, 10, 15, 20, 25) to the total aluminum melt were added and pressed into the aluminum melt with a campanulate graphite mantle, because they tended to float on the surface of the aluminum melt for their low density comparing with aluminum. During the melt in situ reaction, the impulse magnetic field producing device (WY1600) was turned on and the frequency was fixed at 25 Hz and the magnetic current intensity was 150 A. After 20 min, the melt was degassed, slag removed and refined, then was poured into special mould with 14 mm inside diameter. After cooled to the room temperature in air,

---

* Corresponding author. Tel.: +86 511 8791947; fax: +86 511 8791947.
E-mail addresses: zsl@ujs.edu.cn, zhaoyt@ujs.edu.cn (Y.-T. Zhao).

0925-8388/$ – see front matter © 2006 Elsevier B.V. All rights reserved.
doi:10.1016/j.jallcom.2006.04.038

Table 1
Nominal composition of the experimental $Zr(CO_3)_2$ powder

Substance	Content (wt.%)
$Zr(CO_3)_2$	≥ 99.97
SiO_2	≤ 0.01
Al_2O_3	≤ 0.003
Fe_2O_3	≤ 0.002
Na_2O	≤ 0.01
TiO_2	≤ 0.005
SO_4	≤ 0.001

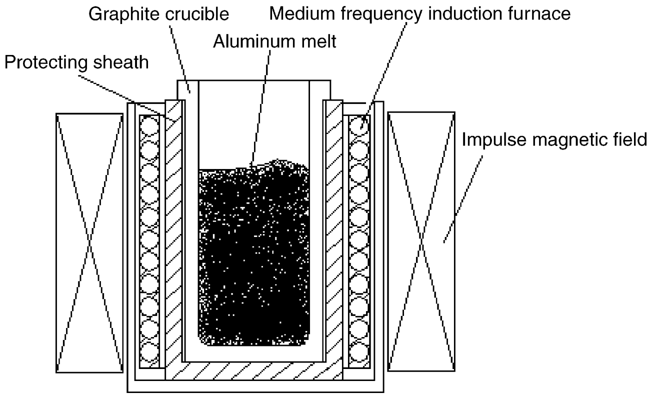

Fig. 1. Schematic diagram of experiment setup.

the specimens were cut two parts, the small one was used for XRD and SEM analysis and the large one for mechanical properties testing.

X-ray diffractometer (Dmax2500PC) using Cu Kα radiation was used to determine phase component of the as-prepared specimens; scanning electron microscopy (SEM, JOEL-JXA-840) and transmission electron microscopy (TEM, JEOL-JEM-2000) were used to analysis the microstructure of the as-prepared ones. The particle size of the in situ reinforcement phase was characterized by an image analyzer. Tensile properties test of the specimens with a gauge diameter of 6.35 mm (0.25 in.) and length of 25.4 mm (1.0 in.) were carried out at room temperature by a computer-controlled electronic tensile testing machine (DWD-200) at a strain rate $1.67 \times 10^{-4}\,s^{-1}$ according to the ASTM E8 standard. Comparing the as-prepared composites with the pure aluminum (defined $x = 0$), the pure aluminum testing specimens were also prepared in the present experiment. The tensile properties are the average values of three tests at each condition. The fracture surfaces of the as-prepared specimens were observed under SEM.

3. Results and discussion

3.1. Preparation of the composites fabricated from Al–*x* wt.% $Zr(CO_3)_2$ ($x = 5, 10, 15, 20, 25$) systems

The XRD patterns of the composites synthesized from Al–*x* wt.% $Zr(CO_3)_2$ ($x = 5$, 10, 15, 20, 25) systems by above method are shown in Fig. 2. It consists of Al, Al_2O_3 and Al_3Zr three phases according to Refs. [19–21], respectively. As shown in Fig. 2, it can be seen that with the increase of x from 5 to 25, the phases of the as-prepared composites changed as followed: when $x = 5$, weak intensity lines of Al_2O_3 and Al_3Zr phases were observed; and they became stronger with the increase of x to 25. Especially, when $x = 20$, 25, the strong peaks of Al_2O_3 and Al_3Zr phases were observed. This is attributed to the increasing additional amount of inorganic salt $Zr(CO_3)_2$ to the molten aluminum. The relative variation of the in situ Al_2O_3 and Al_3Zr phases affect the overall mechanical properties of the aluminum matrix composites.

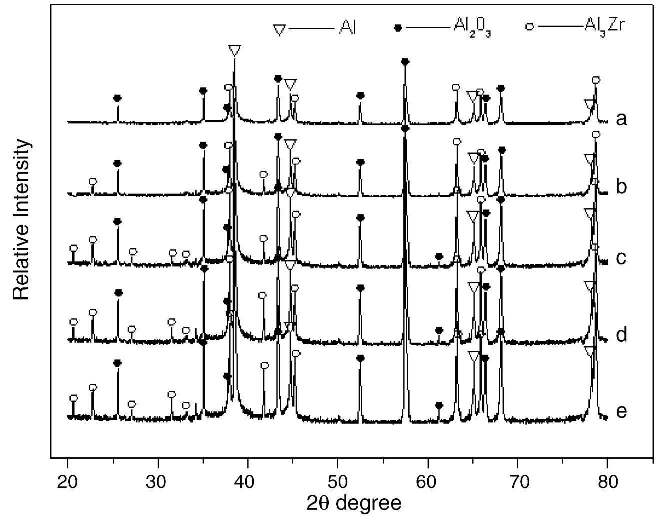

Fig. 2. XRD patterns of the composites synthesized from Al–*x* wt.% $Zr(CO_3)_2$ ($x = 5$, 10, 15, 20, 25) systems: (a) $x = 5$; (b) $x = 10$; (c) $x = 15$; (d) $x = 20$; (e) $x = 25$.

In the Al–$Zr(CO_3)_2$ system, some chemical reactions take place in the aluminum molten liquid at 1173 K. The formations of the in situ Al_2O_3 and Al_3Zr phases are described by the following reactions:

$$Zr(CO_3)_2 \rightarrow ZrO_2 + 2CO_2\uparrow \tag{1}$$

$$3ZrO_2 + 4Al_{(l)} \rightarrow 3[Zr] + 2Al_2O_3 \tag{2}$$

After reactions (1) and (2), the Zr reduced from the reaction (2) then reacts with $Al_{(l)}$ to form Al_3Zr according to the

Table 2
The expressions and calculated values of the standard Gibbs free energy of ZrO_2, Al_2O_3, Zr and Al substances

Substance	ΔG°_T(J/mol)	$\Delta G^\circ_{1173}(T = 1173\,K)$(J/mol)
ZrO_2	$-1082151.4 + 198.52T$	-849287.44
Al	$-5609.9 - 11.35T$	-18923.45
Al_2O_3	$-1675285.5 + 329.24T$	-1289086.98
Zr	$-8308.6 - 11.23T$	-21481.39

Table 3
The values of tensile strengths (σ_b), yield strengths (σ_s) and elongations (δ) for pure aluminum ($x = 0$) and the as-prepared aluminum matrix composites

x	σ_b (MPa)	k_b	σ_s (MPa)	k_s	δ (%)	k_δ
0	78.0	1.000	42.0	1.000	59.8	1.000
5	97.6	1.252	69.2	1.648	38.7	0.647
10	118.4	1.518	87.4	2.081	34.2	0.572
15	139.8	1.792	118.9	2.831	28.6	0.478
20	167.8	2.151	138.5	3.298	20.9	0.349
25	159.3	2.042	133.1	3.169	15.7	0.263